Chapter I

Introduction

"I am the master of my failure… If I never fail how will I ever learn."

-Sir C. V. Raman

1.1 Background

Nanomaterials have gained great importance in the field of science and technology due to their tunable physical, chemical and biological properties with enhanced performance over their bulk counterpart. Nanomaterials are the materials with a length scale of 1-100 nm in at least one dimension [1]. They are categorised on the basis of their size, shape and composition. Nanoscience and nanotechnology are two terms which are used frequently while describing properties and application of nanomaterials. Nanoscience deals with the study of nanoscale matter as regards, their size and structure dependent properties [2]. In contrast, nanotechnology term is used in manipulation and control of matter in the nanoscale dimension for their various industrial and biomedical applications [3]. Nanotechnology, to a great extent, involves most of the branches of science and technology: physics, chemistry, biology, engineering, computer science and technology.

In modern times, the concept of nanotechnology was first coined by Prof. Richard Feynman of CalTech in his lecture delivered in 1959, in one of the sessions of the American Physical Society. In his lecture called "There's plenty of room at the bottom", for the first time, the possibility of creation of nanostructured materials using atoms as the building particles was introduced [4]. The term 'nanotechnology' was introduced before the scientific community by Japanese scientist Prof. Norio Taniguchi. In his lecture at the International Conference on industrial production in Tokyo in 1979, he discussed the processing principles of materials with nanometer dimensions quite accurately [5]. The ideas regarding the prospects of nanosized materials were put forward by Feynmann and written in a science fiction by K. Eric. Drexler in his book "Engines of Creation: The Coming Era of Nanotechnology" published in 1986 [6]. In the second half of 1980s to the early 1990s, numerous discoveries and inventions were made which led to the foundation of further development of

nanotechnology [7, 8]. Two of such path breaking inventions were scanning tunnelling microscopy (1982) and atomic force microscopy in 1986 [8]. These inventions allowed the scientists to witness individual atoms for the first time. Since then, the development of nanotechnology started to expand all over the world, as evidenced from the number of publications, as well as practical applications (industrial products, designs, concepts etc.) which have increased quite rapidly.

The properties of nanomaterials, such as, optical, mechanical, magnetic, electrical etc. are different from their bulk counterpart as a result of quantum confinement effect [9]. Based on their confinement principles, the nanomaterials can be classified into zero dimensional (0D), one dimensional (1D), two dimensional (2D), and three dimensional (3D) materials [10]. Two dimensional materials are confined in one direction, one dimensional materials are confined in two directions while zero dimensional materials are confined in all the three directions. If nature of confinement is n and number of direction is d then, $n + d = 3$ (n, d = 0, 1, 2, 3).

With relevance in almost every field of our day to day life, nanotechnology has made tremendous impact in the areas of communication, computing, textiles, cosmetics, sports, therapy, automotives, environmental monitoring, fuel cells and energy devices, water purification, food and beverage industry, etc. [7].

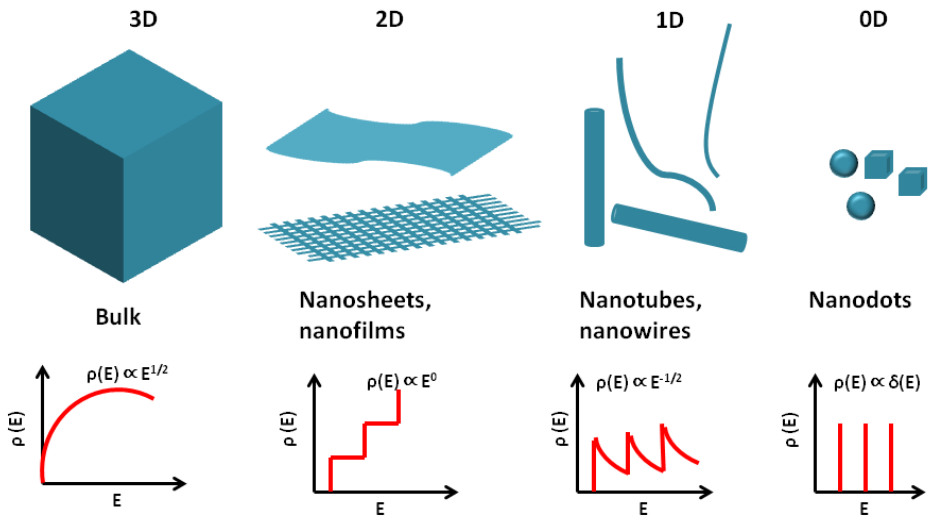

Figure 1.1: Schematic representation of the density of states vs energy of 3D, 2D, 1D and 0D nanomaterials.

1.2 Chalcogenides and transition metal dichalcogenides

Conventional chalcogenides (Metal chalcogenides), are the materials which contain at least one chalcogen (S, Se, Te, Po) anion bonded to at least one electropositive element [11]. Nanostructured metal chalcogenides have attracted the researchers across the globe because of their significant applications in the field of energy storage including fuel cells, solar cells, light emitting diodes, sensors, supercapacitors etc. [12-15]. Depending on the number of chalcogen atoms, metal chalcogenides can be classified as monochalcogenides (CdS, ZnS, ZnSe, MnSe, PbS etc.)[16, 17], dichalcogenides ($MoSe_2$, WS_2, $TaTe_2$ etc.)[18], trichalcogeindes (MoS_3, $NbSe_3$ etc.) [19] and tetrachalcogendes (VS_4 etc.) [20]. Metal chalcogenides are basically semiconductors with a bandgap in the range 1-3 eV.

Dimensionality plays a very important role in the field of material science. Two dimensional materials are the substances having a thickness of few nanometers or less. In a two dimensional material, the movement of electrons inside it is restricted to two directions only. The importance of two dimensional materials was practically realized soon after the discovery of graphene. The isolation of graphene from graphite was first done by Geim and Novoselov in the year 2004 [21]. This discovery is regarded as a major breakthrough in the

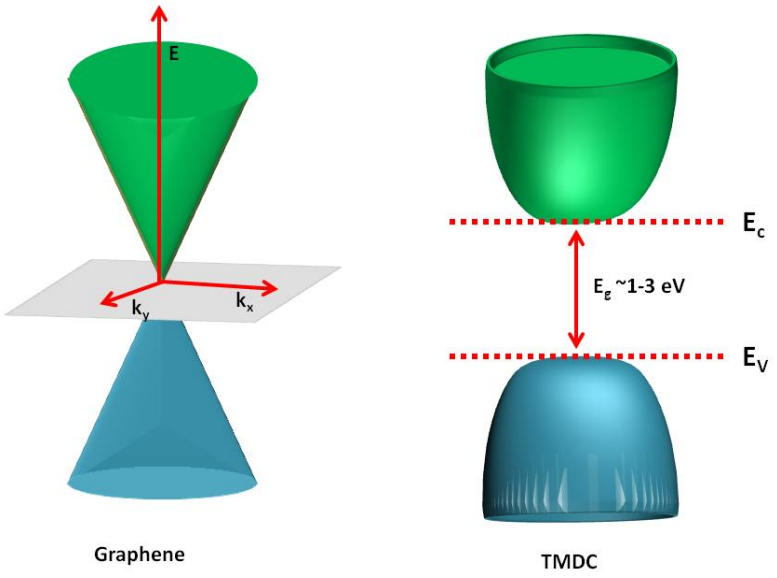

Figure 1.2: Schematic representation of band gap of graphene and TMDC systems.

field of material science. Graphene possesses several exciting properties, like high electron mobility, enhanced electronic and mechanical properties, low density, high surface area and massless Dirac fermions [22-26]. All these extraordinary properties, make graphene a suitable candidate for various applications, such as, transparent electrodes, energy storage devices, solar cells, wearable devices and catalytic agents [27]. But pristine graphene is considered as a semimetallic material with zero bandgap and its intrinsic inversion symmetry strongly suppresses the spin-orbit coupling (SOC). This limits the use of pristine graphene in switching devices [28]. However performing some surface engineering, graphene can give rise to opening of bandgap but doing would reduce carrier mobility drastically. Therefore, the search for appropriate 2D materials began soon after the discovery of grapheme for intended applications. The 2D transition metal dichalcogenides (TMDCs) are layered materials, like graphene with the chemical composition MX_2, where M stands for the transition metal elements and X for the chalcogen elements [27]. Excluding band gap, in almost every aspect, TMDC materials resemble graphene and referred to as graphene analogous materials. It is to be noted that, groups IV-VII metals only tend to form layered structures and consequently, TMDCs [29]. TMDCs occur naturally in the earth crust therein, but the synthesis of TMDCs, sophistication and related scientific publication started only after 1950s [30]. The first report on synthesis of MoS_2 is obtained through the reduction of MoS_3 for which a high temperature solution based technique was employed [30-32]. The early work on TMDCs can be found between 1960 and 1980s, which were mainly focussed on using TMDCs for catalysis and industrial lubricants [33-35]. Thus, the use of TMDCs started before the discovery of graphene but the idea of using few or monolayered TMDCs is realised much later. These materials form layered structures of the form X-M-X, with the layer of metal atoms sandwiched between the two layers of chalcogen atoms. The interlayer bonding among the atoms is simply covalent bond while different layers are attached with one another through the weak Van der Waal bonding [28].

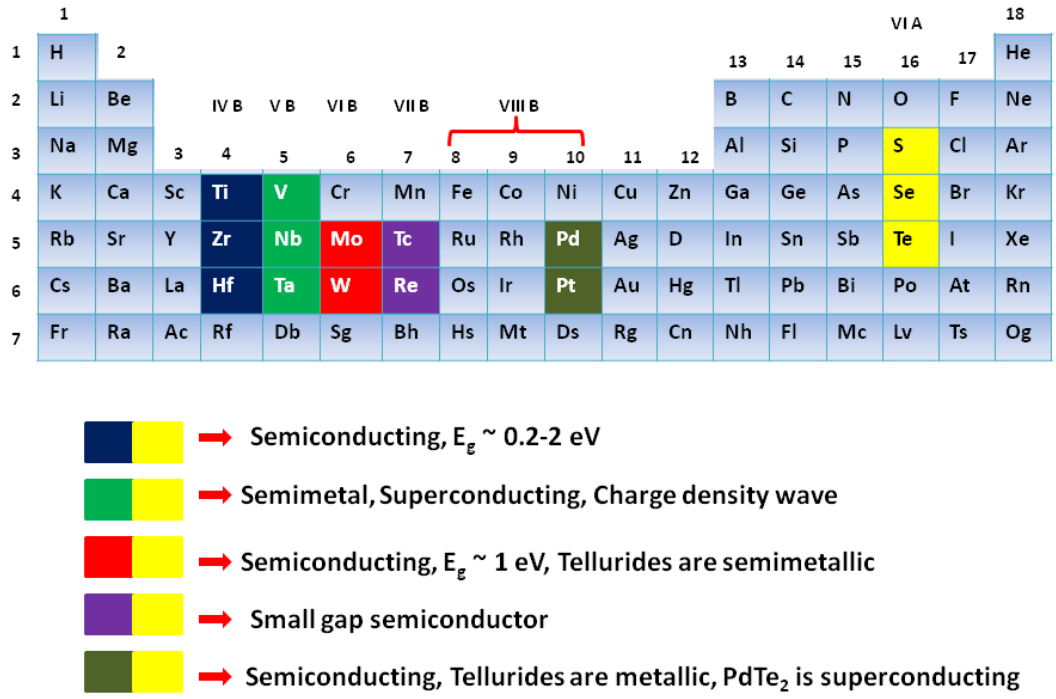

Figure 1.3: Periodic table showing different groups of TMDC materials.

TMDCs can be found in three common structural polytypes: 2H (hexagonal symmetry, two layers per repeat unit, trigonal prismatic coordination), 3R (rhombohedral symmetry, three layers per repeat unit, trigonal prismatic coordination) and 1T (tetragonal symmetry, one layer per repeat unit, octahedral coordination) [36]. The electronic properties of TMDCs range from insulators (HfS_2), semiconductors (MoS_2, WS_2), semi metals (WTe_2) to metals (NbS_2, VSe_2). Some of the TMDCs like $NbSe_2$, TaS_2 exhibit superconductivity and charge density waves at low temperature [27]. The wide range of electronic structures of 2D TMDCs makes them excellent candidate for the electronic and optoelectronic devices. These materials also find their applications in the field of catalysis due to the strong correlation between the electronic and catalytic properties [27]

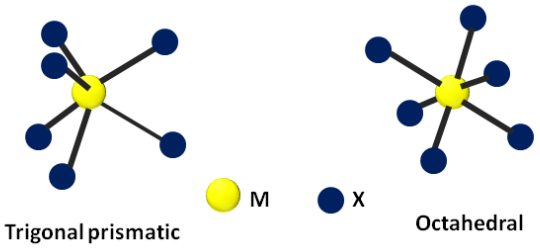

Figure 1.4: Schematic representation of trigonal and octahedral coordination.

Due to high anisotropy and unique crystal structure, the material properties of TMDCs can be tuned significantly by means of different methods including reduction of dimensions and intercalation etc. For instance, MoS_2 is an indirect bandgap semiconductor in the bulk form. But it becomes a direct bandgap (1.9 eV) semiconductor when reduced to monolayer form [37]. Because of weak interlayer Van der Waal bonding of TMDCs one layer can slide over the other and this feature would make them a perfect candidate for solid lubrication [38]. The use of TMDC materials covers many technologically important fields, such as, electronics and optoelectronics, catalysis, energy storage devices, solid lubrication, gas sensors etc.[28].

Among different members of TMDCs, MoS_2 and WS_2 have shown excellent properties and have potential applications in various fields such as, solid-state lubricants, heterogeneous catalysis, separation membranes and energy storage devices. Both MoS_2 and WS_2 have an analogous structure and similar physical and chemical properties. However, WS_2 has not been studied extensively as compared to MoS_2. Whereas, the natural abundance of W is similar to that of Mo, but the industrial consumption of Mo is currently higher which may offer threat to mineral resources [39]. Therefore, to encourage a balance view, W based layered systems can also be recommended for future industrial applications. Moreover, W has several advantages over Mo, such as, less price, low toxicity, high stability etc. [39].

Tungsten disulphide (WS_2) is a semiconducting TMDC material where the W atoms are sandwiched between two layers of S atoms with strong in-plane

bonding. Different layers are attached to one another via weak van der Waal interactions. Depending on the arrangements of S atoms, WS_2 layers show two distinct symmetries, viz. 1T phase (octahedral O_h) and 2H phase (trigonal prismatic D_{3h}) which result in distinctly different properties. The 2H phase is found to be more stable than the 1T phase. The WS_2 has drawn attention owing to its tremendous application in the field of hydrogen storage, microelectrode material, solid lubrication, photocatalysis etc [40-42]. Likewise, all other TMDCs, WS_2 also undergoes a transformation from indirect to direct band gap type on decreasing the number of layers. This transition from indirect to direct bandgap and an increase in bandgap energy are quite evident as a consequence of respective changes in photoconductivity, absorption spectra and photoluminescence response. Being an important member of TMDC family, WS_2 could absorb light over a wide range of electromagnetic spectrum: visible, infrared, ultraviolet and near infrared, allowing it for self-excitation under light irradiation [43].

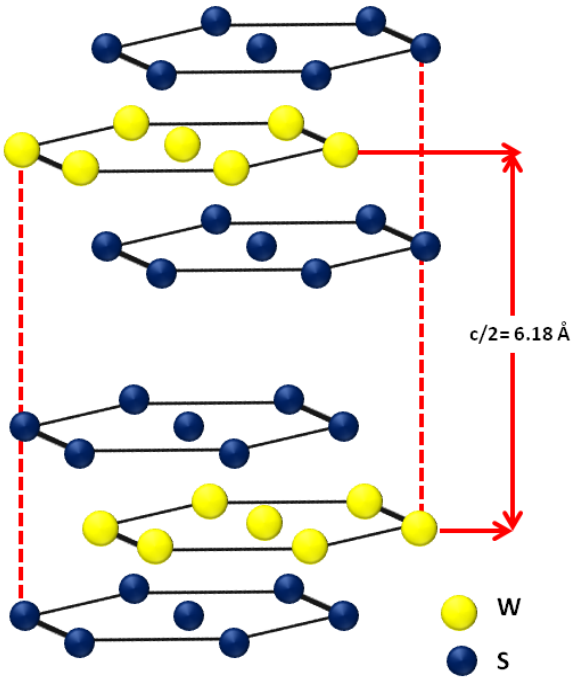

Figure 1.5: Schematic representation of the arrangements of atoms in WS_2.

Visible light responsive photocatalyst based on nanostructured WS_2 have found a broader range of applications, while comparing with the traditional photocatalyst, such as, wide band gap TiO_2, ZnO and SnO_2 , which are active only under UV light illumination [43].

Apart from having a wide range of optical and optoelectronic properties, WS_2 also show high mechanical strength. In particular, WS_2 nanotubes and inorganic fullerene (IF) type WS_2 nanoparticles have demonstrated specific mechanical properties, associated with their unique structure [44]. WS_2 can also serve as an excellent solid lubricant, in the form of additives to lubrication fluids, greases and for self lubricating coatings [45].

WS_2 can be found in different morphologies: nanowires, nanotubes, nanoflowers, nanoribbons, nanosheets and inorganic fullerene type (IF) WS_2 nanoparticles. Among these, WS_2 nanosheets and IF-WS_2 nanoparticles (Fig. 1.6) are considered to be very important owing to their potential applications in the field of catalysis, microelectrode design and solid lubrication [46, 47].

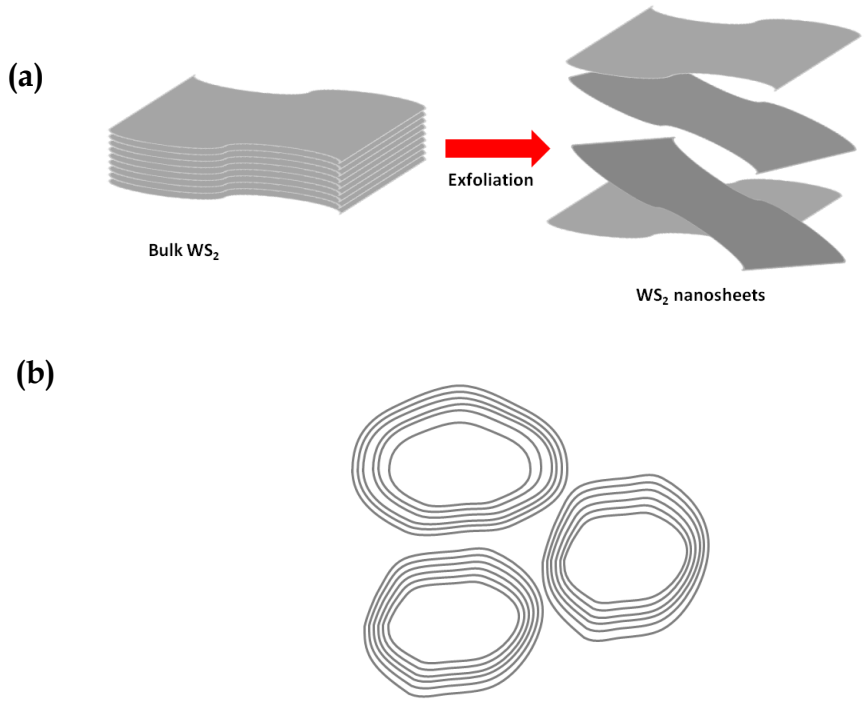

Figure 1.6: Schematic diagram of (a) bulk WS_2 material exfoliated to nanosheets, (b) IF-type WS_2 nanoparticles.

1.3 Photocatalytic activity of nanomaterials/TMDC

Photocatalysis is a process in which the rate of a chemical reaction is enhanced by a substance (called, catalyst) in presence of light. This process is effectively used to degrade harmful chemicals and industrial wastes which are hazardous to surrounding environment and the ecosystem at large [48]. The water waste released from the industries as byproducts contains harmful dyes and extremely hazardous chemicals, which cause threat to the aquatic life, animals and also human beings [48, 49]. So, it is very important to degrade those harmful pollutants into harmless entities which could provide safeguard to the environment we live in. Several methods have been used for the decomposition of the pollutants like chemical oxidation, activated carbon adsorption, biological treatment, etc [50-52]. But they are not as effective as the photocatalysis method. The photocatalytic activity of a material is its ability to degrade a pollutant. The nanomaterials, like TiO_2, CdS, WO_3, SnS and ZnO are extensively used as nano-photocatalysts [53-57]. The photodegradation process is found to depend on several parameters, like amount of the photocatalyst, temperature of the reaction medium, pH of the solution, irradiation time, optical band gap and surface area of the photocatalyst [58].

It is found that, TMDC could absorb light over a wide range of electromagnetic spectrum: visible, infrared, ultraviolet and near infrared, allowing it for self-excitation under light irradiation [46]. The visible light responsive photocatalyst based on nanostructured TMDC have found a broader range of applications, comparing with the traditional photocatalyst, such as, TiO_2 and ZnO with a wide band gap, which are active only under UV light [43]. The two dimensional (2D) TMDC nanosheets posses a higher surface area and hence, a higher surface-to-volume ratio, which help increasing active sites and eventually become responsible for promotion of interfacial charge transfer of photo-induced electron-hole (*e-h*) pairs [59, 61].

1.4 Mechanical and tribological properties

Now it is established that, owing to quantum size effects and enhanced surface reactivity, nanomaterials warrant much improved physical properties as compared to their bulk counterparts. In the past, as per as physical properties are concerned most of the studies were focussed on either optical or electronic properties. However, excessive discussion on mechanical aspects is limited in existing literature. It has been reported that, nanomaterials exhibit enhanced mechanical properties, as compared to their bulk counterpart and this enhancement was attributed to the structural perfection of the materials [62]. Not surprisingly, nanomaterials of different morphologies, such as nanoparticles, nanotubes, nanowire etc. show substantially improved mechanical properties. Several factors/parameters have direct influence on the mechanical properties, such as surface structure, porosity, synthesis methods, etc. [63]. The 2D materials are known to have good mechanical properties, inspite of their ultrathin structure [64]. This has drawn ample interest among material scientists and researchers. Among 2D TMDC materials, WS_2 was studied quite extensively. WS_2 nanotubes and inorganic fullerene (IF) type WS_2 nanoparticles have demonstrated specific mechanical properties, associated with their unique structures [44]. For example, IF-WS_2 nanoparticles are shown to withstand shockwaves of up to 25 GPa and WS_2 nanotubes up to 21 GPa, thus implying superiority features over multi-wall CNTs [65]. During the shockwave treatment, no significant structural degradation, or phase change was observed. These materials comprise of the strongest cage molecules known today and thus making them suitable candidate for shielding in cars, and perhaps, can be used as additive to strengthen construction of materials [66]. It was also found that, adding a small amount of WS_2 nanopowder to a polymeric matrix can substantially improve the linear and nonlinear mechanical properties of the matrix [67, 68]. These properties include tensile strength, toughness, modulus of elasticity, elongation, hardness etc. One of the methods to predict such mechanical properties is the stress-strain relationship. The schematic fig. of a typical stress strain curve is shown in Fig.1.7.

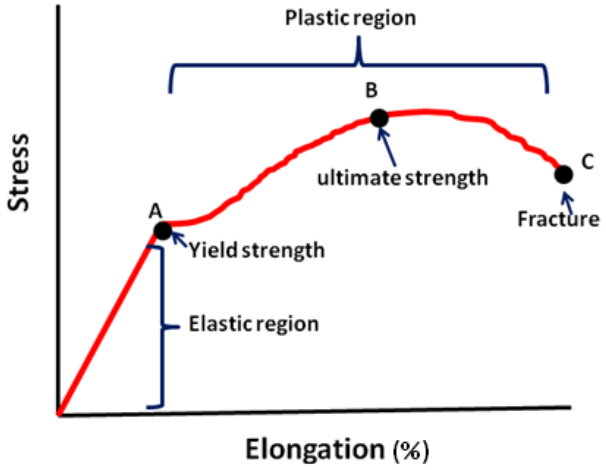

Figure 1.7: Schematic representation of stress-strain curve, showing elastic and plastic regions.

Friction is the resistance offered when two surfaces in contact move relative to each other. Friction results in the loss of a large quantity of mechanical energy. On the other hand, wear leads to the failure of machinery parts of a system. It is known that, one third of the energy is consumed by friction and about 80% of the failure of machine parts is caused by wear [38]. From the beginning of human civilization, efforts are being made to reduce the friction and wear. Traditionally, the use of oil is quite convenient to reduce the friction and wear [38].

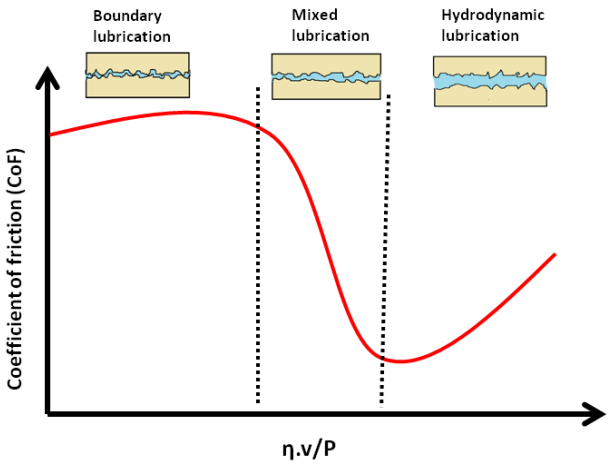

Figure 1.8: Schematic representation of Stribeck curve.

However, oil doesn't play an effective role at high temperature and pressure conditions. With the development of surface engineering technology, different liquid and solid lubrication techniques have been employed in order to reduce the frictional behavior of the mechanical parts [38]. However solid lubrication always finds an upper hand in comparison to the liquid lubrication technique. There are many reports of addition of nanoparticles as solid lubricants to improve the tribological properties of pure oil and grease [38, 69]. Nanoparticles that have been employed as solid lubricants are mostly graphite, graphene, and MoS_2 and CNTs [38].

Friction behavior can be analyzed with the Stribeck curve, which describes the friction coefficient as a function of the combined variables of the rotation speed, normal force, and the viscosity of the lubricant. Briefly, the Stribeck curve presents the relationship between the friction coefficients and lubrication conditions, as shown in Fig. 1.8. Regions I, II and III in the Stribeck curve correspond to hydrodynamic lubrication, boundary lubrication, and mixed lubrication, respectively [70]. The hydrodynamic lubrication regime is mainly influenced by the properties of the lubricant film, whereas the boundary lubrication regime is influenced by material properties and surface interactions between the contacting surfaces. The mixed lubrication regime becomes complicated due to the existence of combined effects between the boundary lubrication and hydrodynamic lubrication. Generally the minimum friction coefficient appears in the mixed lubrication regime [70].

1.5 Effect of ion irradiation on nanomaterials

When a solid is irradiated with energetic electron or ion particles, it leads to the creation of atomic defects in the targets and modifies the properties of the solid at large [71]. Defect modified properties are not only important from fundamental studies point of view but also from the application point of views. Reports have shown that ion, electron and high energy photon irradiation can be

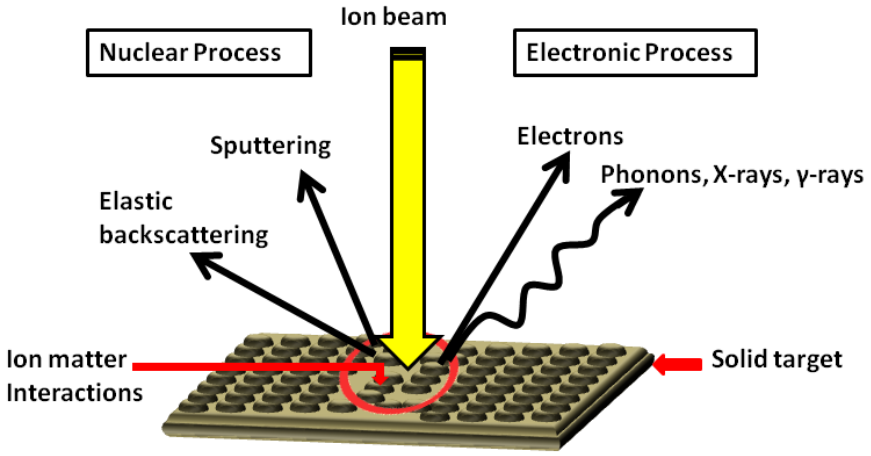

Figure 1.9: Schematic representation of different processes occur during ion matter interaction.

employed to tune mechanical, optical, electronic and magnetic properties of the nanostructured materials [72-76].

When an energetic particle, *viz.*, an electron or ion interacts with a solid, it collides with the electrons and nuclei of the target and transfer the projectile energy to the target atoms (Fig. 1.9). The incident ion during its passage through the target, continuously lose its energy by elastic and inelastic collisions with atoms in the target materials. The net energy loss over a depth x, dE/dx basically has two components as follows [77]:

$$dE/dx = (dE/dx)_{\text{electronic}} + (dE/dx)_{\text{nuclear}} \qquad (1.1)$$

$$S = S_e + S_n$$

The electronic energy loss, S_e arises due to the inelastic collision of the incident ions with the electronic subsystem in the target. The electronic energy loss dominates at higher energy (typically > 100 keV/amu) of the incident ions. On the other hand, the nuclear energy loss, S_n appears as a consequence of the ballistic collisions between the ion and the nuclei of the target, so that the kinetic energy of the colliding ion is partly transferred to the target atom as a whole. The nuclear energy loss is found to dominate at low energy (typically, <10 keV/amu) of the incident ions. Energetic ions play a very important role in the development of nanostructures. Ions of different energy regimes have different

roles in the modification of the nanomaterials [78]. Low energy ions (<1 keV) have been used for the growth of nanoparticle thin films via implantation and also in the development of nanoripples and defects. A few 100 keV ions are used to implant the desired nanoparticles in a given matrix. On the other hand, energetic heavy ions are being used for the growth of nanostructures, phase transformation and structural modifications [78]. The modifications observed in the materials as a result of energetic ion interaction can be explained on the basis of two basic models thermal spike model and Coulomb explosion model [78]. In thermal spike model, ion tracks are formed as a result of the transfer of energy to the lattice through electron-phonon coupling leading to the increase of local temperature [78]. The formation of ion tracks in metallic nanoparticles (eg. Au nanoparticles) as a result of irradiation with high energetic ions can be explained using this model [77]. Whereas, in Coulomb explosion model, the material modification takes place by ionization of the atoms along the path of the ions and subsequent action of coulomb repulsive force [78].

1.6 Motivation

After an extensive literature survey on layered materials, with emphasis upon tungsten disulphide (WS_2) nanosystems, we realized its importance in terms of its existing properties, characteristics and future scope. Despite the fact that, several groups are actively engaged with focused objectives, there is scope for improvement and a lot more to explore. Know that, different morphologies of WS_2 have both advantages as well as limitations prior to their recommendation in real life applications. In this backdrop, herein, we have concentrated on the synthesis principles and basic characterization of WS_2 nanosystems, while focussing upon photocatalytic efficiency, Photoluminescence response and mechanical and tribological features of the system. Special emphasis is made on the low energy ion irradiation aspects of the systems under study.

1.7 Thesis objective and structure

In this work, we have concentrated on TMDC system, specifically tungsten disulphide (WS_2) system. We have synthesized WS_2 nanosystem with different morphologies, *viz.* fullerene (IF) type WS_2, WS_2 nanosheets and carbon dot (C-dot) WS_2 nanohybrid system. Apart from studying their optical property, we have also investigated the photocatalytic efficiency of these synthesized system using harmful target dyes.

In this thesis, we have presented data, facts, and phenomena concerning WS_2 system which is distributed in seven chapters, followed by appendices and addenda. The *Chapter I* deals with the background, literature survey, motivation behind the work, highlighting the thesis objectives towards the end.

In *Chapter II*, we have discussed the synthesis routes and techniques that are employed in the preparation of WS_2, with different morphologies. A two-step hydrothermal method has been employed for processing of IF-WS_2 nanoparticles. And, for the production of WS_2 powder, a single-step hydrothermal process is attempted and then, exfoliated into its nanosheets with the help of repeated ultrasonication. The structural, morphological, optical and vibrational characteristics of the as-prepared systems are studied. The formation of hexagonal WS_2 is confirmed from the XRD analyses. TEM micrographs confirm the morphologies of IF type WS_2 nanoparticles and nanosheets. The EDX micrographs gave evidence of the presence of the elements W and S in the prepared samples. A blue shift of the Raman modes E_{2g}^1 and A_{1g} in the WS_2 sheets compared to WS_2 powder has given adequate clue of exfoliation. Again, the BET analysis shows the increase in specific surface area in the exfoliated nanosheets than the WS_2 powder. As for the synthesis of WS_2/C-dot hybrid system, we have used orange as the natural source of carbon, and decorated over the WS_2 nanosheets with the help of progressive hydrothermal route, which could be affirmed from the TEM micrographs.

Chapter III deals with the Raman and photoluminescence studies of WS_2/C-dot nanohybrid system. The nanohybrid system was found to exhibit excellent fluorescence property, highly tunable with the excitation wavelength. The PL response of the WS_2/C-dot hybrid system displayed a rise, because of the presence of the fluorophore like C-dots. This phenomenon has been attributed to models related to surface traps and electronegativity of heteroatoms. The Raman spectrum of the WS_2/C-dots hybrid nanosystem offered a marginal shifting of E^1_{2g} and A_{1g}; towards lower frequency side along with the evolution of two additional peaks, assigned to the *D* and *G* bands of the graphitic system. This shifting of the Raman modes is ascribed to the strong interaction between the C-dots and WS_2 nanosheets, which can strengthen both in-plane and out-of-plane effective restoring forces acting on them.

In *Chapter IV,* we have discussed the photocatalytic efficiency of our synthesised systems. Considering IF-type WS_2 nanoparticles and WS_2 nanosheets as nano-photcatalysts, we have chosen malachite green (MG) as the target dye and evaluated their photocatalytic activity under both UV and visible light illumination. For WS_2/C-dot hybrid system, we have chosen MG and methyl orange (MO) as the target dye, and evaluated the photocatalytic efficiency under visible light illumination. It was found that among IF-type WS_2 nanoparticles and nanosheets, the nanosheets showed a better photocatalytic response under both UV and visible light. Under visible light, photocatalytic efficiency is seen to be better than that under UV light in both the cases. The enhanced photocatalytic efficiency in case of WS_2 nanosheets is because of the higher surface area of the sheets than that of the IF-nanoparticles. Thus, the nanosheets provide more active sites for the photocatalytic reaction to occur. In case of WS_2/C-dot nanohybrid system, the degradation of MG dye is observed to be more than the MO dye. It is because the absorbance peak (~617 nm) of MG dye falls in the red part of the visible spectrum. On comparing the three systems, we can say that WS_2/C-dot nanohybrid system offers maximal degradation of 91% in 60 min under visible light illumination using MG as the target dye. Using

the same conditions, the degradation values are found to be 86% and 71% for the nanosheets and IF- type WS_2 nanoparticles. The difference in the degradation values of the above for the bare WS_2 nanosheets and the nanohybrid catalysts arises because of the presence of the C-dots in the hybrid material. The C-dots play an important role in enhancing the photoactivity of the 2D WS_2, which can be explained by the physisorption process of the dye onto the WS_2 flakes.

Chapter V highlights the structural, thermogravimetric, mechanical and rheological properties of IF-type nano-WS_2/PVA composite systems. Apart from these properties, wettability features have been studied for the nano-composite system. As for the preparation of PVA films, 3 g of polyvinyl alcohol (PVA) (low molecular weight, ~11,000 Loba Chemie) is dissolved in 100 mL DI water at a temperature of 80°C, for 4 h. After cooling down to room temperature, as-synthesized WS_2 nano powder is added to the PVA solution under vigorous stirring (~350 rpm), followed by ultrasonication (frequency~50 kHz) for about 1 h, in steps. The blended solution was then spread onto a set of borosilicate glass substrates kept at a temperature of 60°C and in order to help complete evaporation of water, they were left undisturbed for ~12 h. The complete process yielded thick solid films, with homogeneously dispersed IF-type WS_2 nanoparticles. The polyhedral, fullerene like nanostructures of WS_2 are quite evident from TEM imaging. For nanocomposite films, elongation and consequently, Young's modulus of elasticity generally offers an increasing trend with a maximum value for 6 wt% nano-WS_2 loading. Breaking stress also gives an enhanced value from 2.7 to 9.7 MPa without and with 6 wt% loading of nano-WS_2. Moreover, tribological studies have revealed a significantly lowered COF with inclusion of nano-WS_2. Thermally and mechanically stable nanocomposite films also presented excellent hydrophobic response by displaying high CA but reduced CAH. Surface energies of the composite films have been calculated by considering contributions from polar and dispersive parts separately for two reference liquids and the net surface energy varies in the range of 24.7 to 37.5 mJ/m^2..

Chapter VI discusses formation and splitting of stacks of WS_2 nanosheets into a few layers under 80 keV Xe^+ ion irradiation at normal incidence. The micro-morphological, visible emission response, Raman active vibronic modes and wettability features are analysed and discussed, on a comparative basis. Multilayer WS_2 nanosheets have been synthesized using a facile hydrothermal method followed by ultrasonication. In order to perform irradiation experiment, the as- prepared WS_2 product was allowed to impregnate on a teflon pellet. Maintaining a constant beam current of ~2 μA, the fluence was varied as, 1×10^{15} (F_1), 5×10^{15} (F_2), 1×10^{16} (F_3) and 5×10^{16} (F_4) ions/cm^2. The electronic energy loss (S_e) and nuclear energy loss (S_n) of the prepared systems were calculated using the SRIM 2008® software. The AFM images of the irradiated samples exhibit surface topology with numerous hillocks and ripple like structures after incorporation of Xe^+, while destroying the smoothness of the film surface. The Raman study affirms the exfoliation of the nano-systems as a result of irradiation. The Stoke's shift is significantly enhanced as evidenced from the increase in electron-phonon coupling parameter, ($S_p > 1$). A clear hydrophilic to hydrophobic transition, as a result of improved surface roughness, caused by normal ion irradiation has also been witnessed.

Chapter VII summarises the important conclusions drawn from the study. The future scope, applications of our present study is briefly described here.

References

[1] Sudha, P. N., Sangeetha, K., Vijayalakshmi, K., Barhoum, A. Nanomaterials history, classification, unique properties, production and market. *Emerging Applications of Nanoparticles and Architectural Nanostructures*, Pages 341-384, ISBN: 978-0-323-51254-1, Elsevier, 2018.

[2] National Research Council Staff. *Small wonders, endless frontiers: a review of the national nanotechnology initiative*. National Academy Press, Washington, DC, United States, 1st edition, 2002.

[3] Goddard, W.A. III, Brenner, D., Lyshevski, S.E., Iafrate, G. J. *Handbook on Nanoscience, Engineeering andTechnology*. United States, CRC press Taylor and Francis, 2nd edition, 2007.

[4] Feynman, R.P. There's plenty of room at the bottom. *Engineering and Science*, 23(5): 22–36, 1960.

[5] Taniguchi, N. On the basic concept of nanotechnology. *Proceedings of the International Conference on Production Engineering*, Tokyo, 18-23, 1974.

[6] Drexler, K.E. *Engines of creation*. New York: AnchorPress/Doubleday, 1986.

[7] Kroto, H.W., Heath, J.R., O'Brien, S.C., Curl, R.F., Smalley, R.E. C60: Buckminsterfullerene. *Nature*, 318:162-163, 1985.

[8] Binning, G., Rohrer, H. Scanning tunneling microscopy, *IBM Journal of Research and Development*, 30(4):355–369, 1986.

[9] Guo, D., Xie, G., Luo, J. Mechanical properties of nanoparticles: basics and applications, *Journal of Physics D: Applied Physics*, 47: 013001 (25pp), 2014.

[10] Pokropivny, V.V., Skorokhod, V.V. Classification of nanostructures by dimensionality and concept of surface forms engineering in nanomaterial science. *Materials Science and Engineering C, 27:* 990–993, 2007.

[11] Greenwood, N. N., Earnshaw, A. *Chemistry of the Elements*. Oxford:Butterworth-Heinemann, 2nd Edition, 1997.

[12] Gao, M. R., Jiang, J., Yu, S. H. Solution-based synthesis and design of late transition metal chalcogenide materials for oxygen reduction reaction (ORR). *Small*, 8:13–27, 2012.

[13] Lai, C. H., Lu, M. Y., Chen, L. J. Metal sulfide nanostructures: synthesis, properties and applications in energy conversion and storage. *Journal of Material Chemistry*, 22:19–30, 2012.

[14] Yuan, M.D., Mitzi, B. Solvent properties of hydrazine in the preparation of metal chalcogenide bulk materials and films. *Dalton Transactions*, 31:6065–6236, 2009.

[15] Antunez, P.D., Buckley, J.J., Brutchey, R. L. Tin and germanium monochalcogenide IV–VI semiconductor nanocrystals for use in solar cells. *Nanoscale*, 3:2399–2411, 2011.

[16] Cunningham, G., Lotya, M., Cucinotta, C. S., Sanvito, S., Bergin, S. D., Menzel, R., Shaffer, M. S. P., Coleman, J. N. Solvent Exfoliation of Transition Metal Dichalcogenides: Dispersibility of Exfoliated Nanosheets Varies Only Weakly between Compounds. *ACS Nano*, 6:3468–3480, 2012.

[17] Kamat, P. V., Tvrdy, K., Baker, D. R., Radich, J. G. Beyond Photovoltaics: Semiconductor Nanoarchitectures for Liquid-Junction Solar Cells. *Chemical Reviews*, 110:6664–6688, 2010.

[18] Zhang, G. Q., Finefrock, S., Liang, D. X., Yadav, G. G., Yang, H. R., Fang, H. Y., Wu, Y. Semiconductor nanostructure-based photovoltaic solar cells. *Nanoscale*, 3:2430–2443, 2011.

[19] Srivastava, S. K., Avasthi, B. N. Review Preparation, structure and properties of transition metal trichalcogenides, *Journal of Material Science*, 27:3693-3705, 1992.

[20] Pang, Q., Zhao, Y., Yu, Y., Bian, X., Wang, X., Wei, Y., Gao, Y., Chen, G. Ultrafine VS4 Nanoparticles Anchored on Graphene Sheets as a High-Rate and Stable Electrode Material for Sodium Ion Batteries. *ChemSusChem*, 11(4):735-742, 2018.

[21] Novoselov, K.S., Jiang , D., Schedin , F., Booth, T.J., Khotkevich , V.V., Morozov, S.V., Geim, A.K. Two-dimensional atomic crystals. *Proceedings of the National Academy of Sciences U.S.A.*, 102:10451-10453, 2005.

[22] Bolotin, K. I., Sikes, K. J., Jiang, Z., Klima, M., Fudenberg, G., Hone, J., Kim, P. Stormer, H. L. Ultrahigh Electron Mobility in Suspended Graphene. *Solid State Communications,* 146:351–355, 2008.

[23] Civalek, Ö. Elastic Buckling Behavior of Skew Shaped Single-Layer Graphene Sheets. *Thin Solid Films,* 550:450–458, 2014.

[24] Martin, J., Akerman, N., Ulbricht, G., Lohmann, T., Smet, J. H., von Klitzing, K., Yacoby, A. Observation of Electron-Hole Puddles in Graphene Using a Scanning Single Electron Transistor. *Nature Physics, 4*:144-148, 2007.

[25]] Stoller, M.D., Park, S., Yanwu, Z., An, J., Ruoff, R.S. Graphene-Based Ultracapacitors. *Nano Letters,* 8:3498–3502, 2008.

[26] Nair, R. R., Blake, P., Grigorenko, A. N., Novoselov, K. S., Booth, T. J., Stauber, T., Peres, N. M. R., Geim, A. K. Fine Structure Constant Defines Visual Transparency of Graphene. *Science,* 320:1308, 2008.

[27] Chhowalla, M., Shin, H. S., Eda, G., Li, L.-J., Loh, K. P., Zhang, H. The chemistry of two-dimensional layered transition metal dichalcogenide nanosheets, *Nature Chemistry*, 5:263-275, 2013.

[28] Wang, Q. H., Kalantar-Zadeh, K., Kis, A., Coleman, J. N., Strano, M. S. Electronics and optoelectronics of two-dimensional transition metal dichalcogenides, *Nature Nanotechnology*, 7:699-712, 2012.

[29] Late, D.J., Rout, C. S., Chakravarty, D., Ratha, S. Emerging Energy Applications of Two-Dimensional Layered Materials. *Canadian Chemical Transactions*, 3:118-157, 2015.

[30] Eggertsen, F.T., Roberts, R.M. Molybdenum disulfide of high surface area. *Journal of Physical Chemistry,* 63:1981-1982, 1959.

[31] H. Yagoda , H.A. Fales , The separation and determination of tungsten and molybdenum. *Journal of American Chemical Society,* 58:1494, 1936.

[32] Arutyuny, L.A., Khurshud, E.K. *Geochem. Int. USSR* 3:479, 1966.

[33] Wilson, J.A., Yoffe, A.D. The transition metal dichalcogenides discussion and interpretation of the observed optical, electrical and structural properties. *Advances in Physics,* 18:193-335, 1969.

[34] Wieting, T.J., Schlüter, M. *Electrons and Phonons in Layered Crystal Structures.* Springer Netherlands, Dordrecht, 1st edition, 1979.

[35] Motizuki, K. *Structural Phase Transitions in Layered Transition Metal Compounds*. Springer Netherlands, Dordrecht, 1st edition, 1986.

[36] Zappa, D. Molybdenum Dichalcogenides for Environmental Chemical Sensing. *Materials*, 10:1418, 2017.

[37] Kuc, A., Zibouche, N., Heine, T. Influence of quantum confinement on the electronic structure of the transition metal sulfide TS_2. *Physical Review B*, 83:245213, 2011.

[38] Wang, H., Xu, B., Liu, J. *Micro and nano sulfide solid lubrication*. Science Press Beijing and Springer-Verlag Berlin Heidelberg, 1st edition, 2012.

[39] Taylor, T. Abundance of Chemical Elements in the Continental Crust: a New Table, *Geochimica et Cosmochimica Acta*, 28:1273–1285, 1964.

[40] Voiry, D., Yamaguchi, H., Li, J., Silva, R., Alves, D.C.B., Fujita, T., Chen, M.W., Asefa, T., Shenoy, V.B., Eda, G., Chhowalla, M. Enhanced catalytic activity in strained chemically exfoliated WS_2 nanosheets for hydrogen evolution. *Nature Materials*, 12:850-855, 2013.

[41] Rapoport, L., Bilik, Y., Feldman, Y., Homyonfer, M., Cohen, S.R., Tenne, R. Hollow nanoparticles of WS_2 as potential solid-state lubricants. *Nature*, 387:791–793, 1997.

[42] Levi, R., Bitton, O., Leitus, G., Tenne, R., Joselevich, E. Fieldeffect transistors based on WS_2 nanotubes with high current carrying capacity. *Nano Letters*, 13:3736–3741, 2013.

[43] Mishra, A.K., Lakshmi, K.V., Huang, L. Eco-friendly synthesis of metal dichalcogenides nanosheets and their environmental remediation potential driven by visible light. *Scientific Reports,* 5:15718, 2015.

[44] Kaplan-Ashiri, I., Tenne, R. On the Mechanical Properties of WS_2 and MoS_2 Nanotubes and Fullerene-Like Nanoparticles: In Situ Electron

Microscopy Measurements. *The Journal of The Minerals, Metals & Materials Society*, 68:151-167, 2016.

[45] Zhang, X., Xu, H., Wang, J., Ye, X., Lei, W., Xue, M., Tang, H., Li, C. Synthesis of Ultrathin WS_2 Nanosheets and Their Tribological Properties as Lubricant Additives, *Nanoscale Research Letters*, 11:442 page 1-9, 2016.

[46] Sang, Y., Zhao, Z., Zhao, M., Hao, P., Leng, Y., Liu, H. From UV to near-infrared, WS_2 nanosheet: a novel photocatalyst for full solar light spectrum photodegradation. *Advanced Materials*, 27:363–369, 2015.

[47] Greenberg, R., Halperin, G., Etsion, I., Tenne, R. The effect of WS_2 nanoparticles on friction reduction in various lubrication regimes. *Tribology Letters*, 17:179-186, 2004.

[48] Park, Y., Lee, S., Kang, S.O., Choi, W. Organic dye-sensitized TiO_2 for the redox conversion of water pollutants under visible light. *Chemical Communications*, 46(14): 2477-2479, 2010.

[49] Hoffmann, M.R., Martin, S.T., Choi, W., Bahnemann, D.W. Environmental applications of semiconductor photocatalysis. *Chemical Reviews* 95(1):69-96, 1995.

[50] Okano, M., Itoh, K., Fujishima, A., Honda, K. Photoelectrochemical polymerization of pyrrole on TiO_2 and its application to conducting pattern generation. *Journal of the Electrochemical Society*, 134(4):837-841, 1987.

[51] Zeltner, W.A., Hill, C.G., Anderson, M.A. Supported titania for photodegradation. *Chem Tech*, 23:21, 1993.

[52] Mills, A., Davies, R.H., Worsley, D. Water purification by semiconductor photocatalysis. *Chemical Society Reviews*, 22(6): 417-425, 1993.

[53] Cetinkaya, T., Neuwirthová, L., Kutláková, K.M., Tomášek, V., Akbulut, H. Synthesis of nanostructured TiO_2/SiO_2 as an effective photocatalyst for degradation of acid orange. *Applied Surface Science*, 279:384–390, 2013.

[54] Jun, L., Yonghong, N., Jie, L., Jianming, H. Preparation, conversion, and comparison of the photocatalytic property of $Cd(OH)_2$, CdO, CdS and CdSe. *Journal of Physics and Chemistry of Solids*, 70(9):1285–1289, 2009.

[55] Zhang, H., Yang, J., Guo, W., Zhu, L., Zheng, W. Temperature and acidity effects on WO3 nanostructures and gas-sensing properties of WO_3 nanoplates. *Materials Research Bulletin*, 57:260–267, 2014.

[56] Gao, C., Shen, H., Sun, L., Shen, Z. Chemical bath deposition of SnS films with different crystal structures. *Material Letters*, 65:1413–1415, 2011.

[57] Faisal, M., Khan, S.B., Rahman, M.M., Jamal, A., Abdullah, M.M. Fabrication of ZnO nanoparticles based sensitive methanol sensor and efficient photocatalyst. *Applied Surface Science*, 258:7515–7522, 2012.

[58] Kumar, A., Pandey, G. A Review on the Factors Affecting the Photocatalytic Degradation of Hazardous Materials. *Material Science & Engineering International Journal*, 1(3): 00018, 2017.

[59] Zhang, J., Zhu, Z. P., Feng, X. L. Construction of Two Dimensional MoS_2/CdS p-n Nanohybrids for Highly Efficient Photocatalytic Hydrogen Evolution. *Chemistry: A European Journal*, 20:10632−10635, 2014.

[60] Zhu, Y. Y., Ling, Q., Liu, Y. F., Wang, H., Zhu, Y. F. Photocatalytic H_2 evolution on MoS_2-TiO_2 catalysts synthesized via mechanochemistry. *Physical Chemistry Chemical Physics*, 17:933−940, 2015.

[61] Vattikuti, S. V. P., Byon, C., Reddy, C. V., Ravikumar, R. Improved photocatalytic activity of MoS_2 nanosheets decorated with SnO_2 nanoparticles. *RSC Advaces*, 5:86675−86684, 2015.

[62] Guo, D., Xie, G., Luo, J. Mechanical properties of nanoparticles: basics and applications. *Journal of Physics D: Applied Physics*, 47:013001 (25pp), 2014.

[63] Reghunadhan, A., Kalarikkal, N., Thomas, S. Mechanical Property Analysis of Nanomaterials, *Characterization of Nanomaterials*. Elsevier Ltd., 2018.

[64] Kim, J.H., Jeong, J.H., Kim, N., Joshi, R., Lee, G-H. Mechanical properties of two-dimensional materials and their applications. Journal of Physics D: Applied Physics, 52: 083001 (32pp), 2019.

[65] Zhu, Y. Q., Sekine, T., Li, Y.H., Fay, M. W., Zhao, Y.M., Poa, C. H. P., Wang, W. X., Roe, M. J., Brown, P.D. , Fleischer, N., Tenne, R. Shock-Absorbing and Failure Mechanisms of WS_2 and MoS_2 Nanoparticles with Fullerene-like Structures under Shock Wave Pressure. Journal of American Chemical Society, 127:16263-16272, 2005.

[66] Tenne, R. Inorganic nanotubes and fullerene-like nanoparticles. *Journal of Materials Research,* 21(11):2726–2743, 2006.

[67] Zohar, E., Baruch, S., Shneider, M., Dodiuk, H., Kenig, S., Tenne, R., Wagner, H.D. The effect of WS_2 nanotubes on the properties of epoxy-based nanocomposites. *Journal of Adhesion Science and Technology*, 25:1603-1617, 2011.

[68] Reddy, C.S., Zak, A., Zussman, E. WS_2 nanotubes embedded in PMMA nanofibers as energy absorptive material. *Journal of Material Chemistry*, 21:16086-16093, 2011.

[69] Rapoport, L., Leshchinsky, V., Lapsker, I., Volovik, Y., Nepomnyashchy, O., Lvovsky, M., Popovitz-Biro, R., Feldman, Y., Tenne, R. Tribological properties of WS_2 nanoparticles under mixed lubrication. *Wear*, 255:785–793, 2003.

[70] Zhu, D., Wang, J., Wang Q. J. On the Stribeck Curves for Lubricated Counterformal Contacts of Rough Surfaces. *Journal of Tribology*, 137:021501-1-10, 2015.

[71] Krasheninnikov, A.V., Nordlund, K. Ion and electron irradiation-induced effects in nanostructured materials. *Journal of Applied Physics*, 107:071301, 2010.

[72]] Peng, B., Locascio, M., Zapol, P., Li, S., Mielke, S.L., Schatz, G.C., Espinosa, H.D. Measurements of near-ultimate strength for multiwalled carbon nanotubes and irradiation-induced crosslinking improvements. *Nature Nanotechnology*, 3:626-631, 2008.

[73] Kis, A., Csányi, G., Salvetat, J.-P., Lee, T.-N., Couteau, E., Kulik, A.J., Benoit, W., Brugger, J., Fórro, L. Reinforcement of single-walled carbon

nanotube bundles by intertube bridging. *Nature Materials*, 3:153-157, 2004.

[74] Gómez-Navarro, C., De Pablo, P. J., Gómez-Herrero, J., Biel, B., Garcia-Vidal, F. J., Rubio, A., Flores, F. Tuning the conductance of single-walled carbon nanotubes by ion irradiation in the Anderson localization regime. *Nature Materials*, 4:534-539, 2005.

[75] Stahl, H., Appenzeller, J., Martel, R., Avouris, P., Lengeler, B. Intertube Coupling in Ropes of Single-Wall Carbon Nanotubes. *Physical Review Letters*, 85:5186, 2000.

[76] Talapatra, S., Ganesan, P.G., Kim, T., Vajtai, R., Huang, M., Shima, M., Ramanath, G., Srivastava, D., Deevi, S.C., Ajayan, P.M. Irradiation-induced magnetism in carbon nanostructures. *Physical Review Letters*, 95:097201, 2005.

[77] Ziegler, J.F., Biersack, J.P., Littmark, U. *The Stopping and Range of Ions in Matter* Pergamon, New York, 1985.

[78] Avasthi, D.K., Mehta, G.K. *Swift Heavy Ions for Materials Engineering and Nanostructuring*. Springer, Netherlands, 1st edition, 2011.